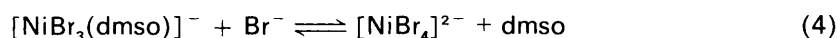
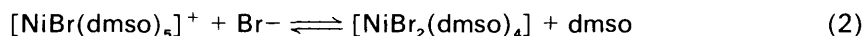


## The Nickel(II)–Bromide System in Dimethyl Sulphoxide: A Detailed Study of the Influences of Temperature and Mole Ratio

Trevor R. Griffiths\* and Nicolas J. Phillips

Department of Inorganic and Structural Chemistry, The University, Leeds LS2 9JT

The bromo-nickel(II) species occurring in dimethyl sulphoxide (dmsO) solutions have been identified from their ligand field spectra and comprise the octahedral complexes  $[\text{NiBr}(\text{dmsO})_5]^+$  and  $[\text{NiBr}_2(\text{dmsO})_4]$ , and the tetrahedral complexes  $[\text{NiBr}_3(\text{dmsO})]^-$  and  $[\text{NiBr}_4]^{2-}$ . The absorption spectra were recorded of solutions at various Br: Ni mole ratios, from 2 to 154, and from room temperature to 170 °C. Within separate temperature and Br: Ni mole ratio ranges five equilibria (1)–(5) were found to predominate. For equilibrium (3) the enthalpy,  $\Delta H$ , varied with Br: Ni mole



ratio, from  $113.1 \pm 1 \text{ kJ mol}^{-1}$  at 8.4 to  $47.2 \pm 1 \text{ kJ mol}^{-1}$  at 154.4, and a plot of  $\Delta H$  vs.  $\log_{10}$  (Br: Ni mole ratio) was linear. For equilibria (4) and (5)  $\Delta H$  values were  $43.7 \pm 1$  and  $-2.7 \pm 1 \text{ kJ mol}^{-1}$ , respectively. It is proposed that equilibrium (4) reverses to (5) at high temperatures, when the dielectric constant of the medium reduces sufficiently to destabilise the doubly charged  $[\text{NiBr}_4]^{2-}$  species. Such a reversal has not previously been reported. The free energy ( $\Delta G$ ) and entropy ( $\Delta S$ ) for equilibria (3)–(5) were obtained. The system is compared with the corresponding chloro system reported earlier. Several parallel general trends were noted, but there are many differences, brought out by this more detailed study.

Some time ago we investigated<sup>1</sup> the influence of temperature and concentration upon chloride–nickel(II) interactions in dimethyl sulphoxide (dmsO). From the absorption spectra we identified the octahedral chloro complexes  $[\text{NiCl}(\text{dmsO})_5]^+$  and  $[\text{NiCl}_2(\text{dmsO})_4]$  and the tetrahedral chloro complexes  $[\text{NiCl}_3(\text{dmsO})]^-$  and  $[\text{NiCl}_4]^{2-}$ . The effect of temperature upon the various equilibria identified as present in solution at various Cl: Ni mole ratios was also studied, and thermodynamic data were calculated<sup>1,2</sup> for the equilibrium  $[\text{NiCl}_2(\text{dmsO})_4] + \text{Cl}^- \rightleftharpoons [\text{NiCl}_3(\text{dmsO})]^- + 3 \text{dmsO}$ . Since then we have examined the formation and stability of chloro, bromo, and iodo complexes of nickel and other metals in a variety of solvents,<sup>3</sup> and noted certain trends. No work has subsequently been reported on bromide–nickel(II) or iodide–nickel(II) interactions in dmsO, and we have therefore returned to this interesting solvent.

A solution of nickel(II) bromide in dmsO is yellow at room temperature, indicating the presence of one or more octahedral complexes, and on heating changes to green then blue, indicating tetrahedral nickel complexes (but no violet colour is seen near its boiling point, as with  $\text{NiCl}_2$  in dmsO). The reaction and symmetry change, as with  $\text{NiCl}_2$ , is reversible, the solution returning to yellow upon cooling. Nickel(II) iodide in dmsO scarcely changes colour on heating and this system is therefore not considered here.

We here report a comprehensive spectroscopic study over Br: Ni mole ratios 2–154 and at temperatures from ambient to 170 °C. The predominant tetrahedral species in solution was  $[\text{NiBr}_3(\text{dmsO})]^-$ , as expected, but the various equilibria identified did not always parallel the chloride–nickel(II) system.

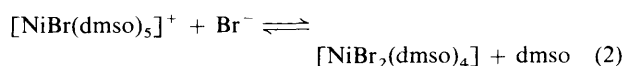
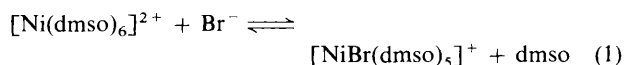
Thermodynamic data were obtained for all these equilibria, in more detail than previously,<sup>1,2</sup> and certain trends were observed.

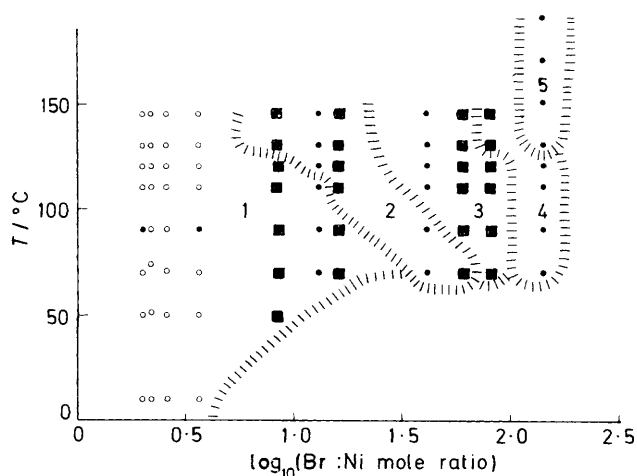
### Experimental

The chemicals used were the purest commercially available. The spectroscopic measurement details given earlier<sup>1</sup> were followed, except that the furnace was based on a design by Boston and Smith,<sup>4</sup> and electronically controlled to within  $\pm 0.2$  °C. Solutions were prepared from a stock solution of nickel(II) bromide and transferred and diluted as necessary using an autopipetter ( $\pm 1.0 \mu\text{l}$ ), Digitron 2000. Lithium bromide was added directly ( $\pm 1 \times 10^{-5} \text{ g}$ ), to increase accurately and successively the Br: Ni mole ratio at constant nickel concentration.

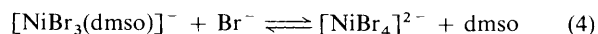
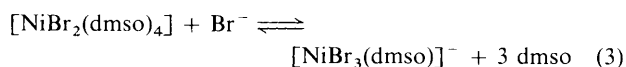
### Results

Figure 1 shows the extensive range of temperatures and Br: Ni mole ratios investigated. The equilibria identified as predominating within various experimental conditions are given in equations (1)–(5). These equilibria proceed to the right with





**Figure 1.** Range of temperature and log Br:Ni mole ratios investigated in dmso. The numbers refer to the corresponding equilibria (1)–(5), within a specific range of experimental conditions. Dashed lines dividing the various single-equilibria regions, being broad, indicate where two or more equilibria co-exist. Symbols indicate conditions (○) under which spectra were recorded; (■) those used in deriving thermodynamic data; (●) those which pertain to the spectra in Figures 2–5

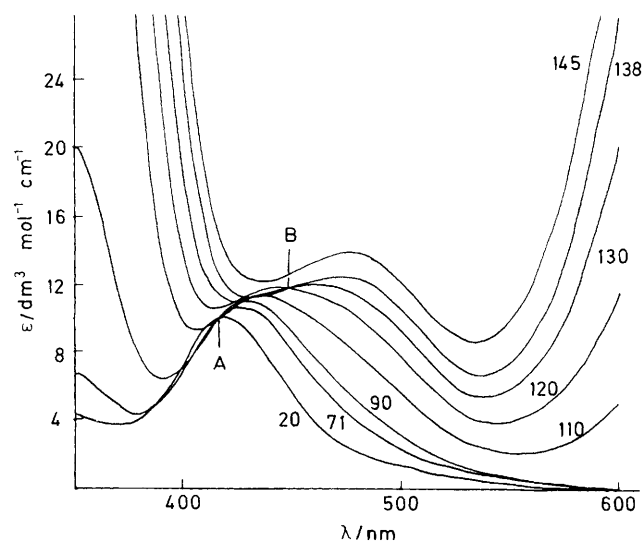


temperature increase, and occur successively as the Br:Ni mole ratio is increased. Figure 1 also indicates, by the broad boundary lines dividing the regions where the various equilibria predominate, that there are, obviously, experimental conditions where two or more equilibria coexist. The absence of data at low temperatures and at high Br:Ni mole ratios is due to the limited solubility of lithium bromide in dimethyl sulphoxide under these conditions.

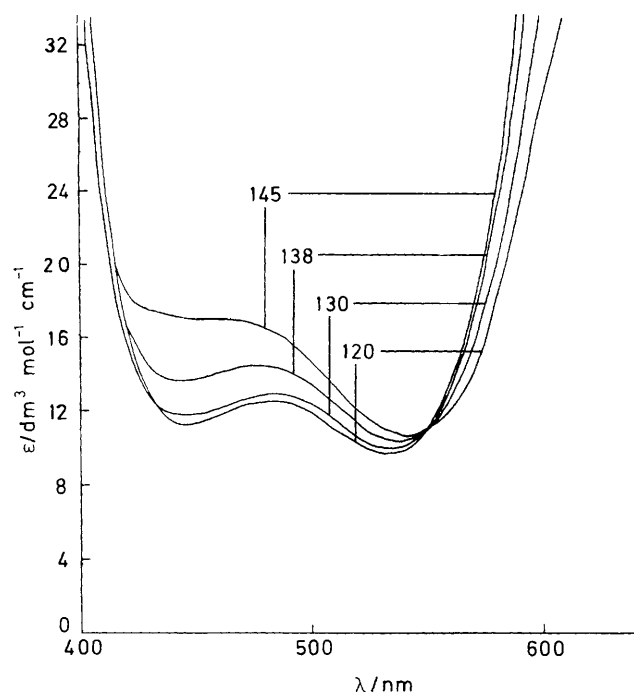
Octahedral and tetrahedral bromo-nickel complexes are readily distinguished; the former have a single transition in the region 400–500 nm and the latter show generally two peaks in the region 650–900 nm. Having two nickel species dominating and in equilibrium within certain experimental conditions is recognised by the appearance of an isosbestic point within a set of spectra recorded under those conditions. This criterion is not absolute, as Smith and Brynstad<sup>5</sup> have shown, but exceptions are rare, and we have therefore assumed that the presence of an isosbestic point confirmed a two-species equilibrium.

*Effect of Temperature Increase.*—(a) At Br:Ni mole ratio of 2.0. When the spectra of solutions of  $\text{NiBr}_2$  and  $\text{NiCl}_2$  in dimethyl sulphoxide were compared, bands associated with tetrahedral species appeared at temperatures in excess of 60 °C in the  $\text{NiCl}_2$  solution, and above 120 °C in the  $\text{NiBr}_2$  system. Since the molar absorbance coefficients,  $\epsilon$ , for tetrahedral species are approximately 10–40 times those of the corresponding octahedral species only a few percent of the nickel species were in the tetrahedral form.

(b) At Br:Ni mole ratio of 13.0. Solutions having around this mole ratio yielded similar spectra to those of anhydrous  $\text{NiCl}_2$  in dmso. Figure 2 shows isosbestic points at 417 and 448 nm. The former point identifies the octahedral–octahedral hexa-solvated/monobromonickel equilibrium, (1). A corresponding datum was not seen in the chloride system,<sup>1</sup> with  $\text{NiCl}_2$ , since chloride forms a much stronger bond to nickel, and thus at low



**Figure 2.** Effect of temperature (20–145 °C) upon octahedral bromo-nickel complexes in a solution of dimethyl sulphoxide containing bromide and nickel(II) at a mole ratio of 13.0. The isosbestic point A, at 417 nm, is identified with the equilibrium  $[\text{Ni}(\text{dmsO})_6]^{2+} + \text{Br}^- \rightleftharpoons [\text{NiBr}(\text{dmsO})_5]^+ + \text{dmsO}$ , while the isosbestic point B, at 448 nm, is identified with  $[\text{NiBr}(\text{dmsO})_5]^+ + \text{Br}^- \rightleftharpoons [\text{NiBr}_2(\text{dmsO})_4] + \text{dmsO}$

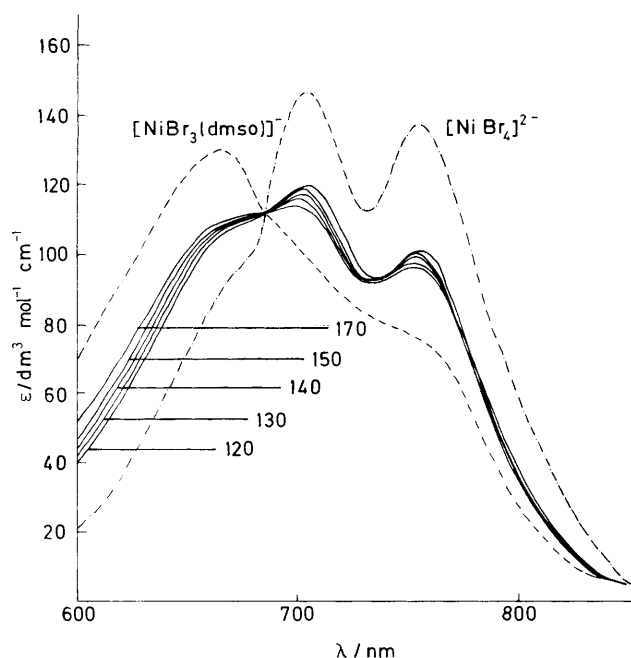


**Figure 3.** Effect of temperature (120–145 °C) upon the absorption spectrum of a dmsO solution containing Br:Ni at mole ratio of 41.1. The wavelength region is restricted to that which shows clearly the isosbestic point at 550 nm, pertaining to the equilibrium  $[\text{NiBr}_2(\text{dmsO})_4] (\text{octahedral}) + \text{Br}^- \rightleftharpoons [\text{NiBr}_3(\text{dmsO})]^- (\text{tetrahedral}) + 3 \text{dmsO}$

temperatures three octahedral nickel species are present in solution. The isosbestic point at 448 nm, not appearing until 120 °C, is therefore comparable with the chloride system point at 440 nm, not appearing until 90 °C, and both points and their experimental conditions are therefore associated with mono-/di-halogeno octahedral complex equilibria. Tetrahedral bromo species could also be detected above 90 °C, but their

**Table 1.** Results obtained during the determination of  $\Delta H$  for the reaction  $[\text{NiBr}_2(\text{dmsO})_4]$  (octahedral)  $\rightleftharpoons$   $[\text{NiBr}_3(\text{dmsO})]^-$  (tetrahedral) in dmsO at Br:Ni mole ratio of 41.1

$T/^\circ\text{C}$	$10^3\text{K}/T$	$\epsilon/\text{dm}^3 \text{ mol}^{-1} \text{ cm}^{-1}$ (at 660 nm)	$10^3[\text{NiBr}_3(\text{dmsO})^-]/$ $\text{mol dm}^{-3}$	$10^3[\text{NiBr}_2(\text{dmsO})_4]/$ $\text{mol dm}^{-3}$	$K$	$\log_{10} K$
70	2.916	2.79	0.685	26.15	0.0262	-1.582
90	2.755	9.76	2.362	24.47	0.0965	-1.015
110	2.611	39.13	9.469	17.36	0.545	-0.263
120	2.545	47.59	11.51	15.32	0.752	-0.124
130	2.481	59.26	14.33	12.50	1.146	0.059
138	2.433	67.83	16.50	10.33	1.587	0.203
145	2.392	70.44	17.04	9.79	1.740	0.241

**Figure 4.** Effect of temperature (120–170 °C) upon a concentrated dmsO solution of LiBr (which is saturated below *ca.* 70 °C), and has a Br:Ni mole ratio of 154.4. The isobestic point at 683 nm belongs to *two* equilibria, between tetrahedral species, *viz.* (4) and (5). {The latter occurs at the temperatures shown here, and the former at temperatures below 120 °C, and also at slightly lower Br:Ni mole ratios. It is therefore impossible to have conditions under which only  $[\text{NiBr}_4]^{2-}$  exists, and similarly, the spectrum of  $[\text{NiBr}_3(\text{dmsO})]^-$  cannot be recorded free from contributions of either or both of  $[\text{NiBr}_4]^{2-}$  and  $[\text{NiBr}_2(\text{dmsO})_4]$ .} The dashed line spectra attributed here to  $[\text{NiBr}_3(\text{dmsO})]^-$  and  $[\text{NiBr}_4]^{2-}$  have been derived and authenticated as explained in the text

concentrations were low and insufficient to negate the isobestic point.

(c) *At Br:Ni mole ratio of 41.1.* This system compared well with the chloro system at a mole ratio of 7.0 except that here tetrahedral species could not be detected at room temperature. An isobestic point was observed above 70 °C at 550 nm (Figure 3), 40 nm higher than that for the corresponding chloro equilibrium.<sup>1</sup> Equilibrium (3), involving the octahedral configurational change, dominates this Br:Ni mole ratio at elevated temperatures.

(d) *At Br:Ni mole ratio of 154.4.* This system is saturated in lithium bromide below about 70 °C. At such high concentrations and temperatures only tetrahedral species could be identified. Equilibrium (4) exhibited an isobestic point at 683 nm (Figure 4), as the temperature was raised to 110 °C, but with further

temperature increase the spectra reversed their behaviour. Above 110 °C equilibrium (5) therefore predominates, as  $[\text{NiBr}_4]^{2-}$  reverts to  $[\text{NiBr}_3(\text{dmsO})]^-$ . No parallel behaviour was observed in the chloro-nickel interaction study,<sup>1</sup> partly because high Cl:Ni mole ratios were not systematically investigated. In the chloro system, ratios of 7.0 showed the presence of both  $[\text{NiCl}_3(\text{dmsO})]^-$  and  $[\text{NiCl}_4]^{2-}$  at room temperature, and largely  $[\text{NiCl}_4]^{2-}$  at the higher mole ratio of 18.2. No isobestic point was observed between  $[\text{NiCl}_3(\text{dmsO})]^-$  and  $[\text{NiCl}_4]^{2-}$  because at these higher ratios significant amounts of both  $[\text{NiCl}(\text{dmsO})_5]^+$  and  $[\text{NiCl}_2(\text{dmsO})_4]$  were still present. A literature survey revealed equilibria which reversed upon concentration change, but none which reversed direction with continued temperature increase.

*Effect of Variation of Br:Ni Mole Ratio at Constant Temperature.*—Addition of bromide at ambient temperature does not produce any blue tetrahedral species before saturation. However, Figure 5 shows the variation in spectra obtained at 130 °C over the complete range of Br:Ni mole ratios used, and includes the spectra of  $[\text{Ni}(\text{dmsO})_6]^{2+}$  and that obtained with  $\text{NiBr}_2$  in dimethyl sulphoxide. With more data isobestic points would be seen, between appropriate Br:Ni mole ratios, but such sets of spectra are experimentally more difficult to obtain.

*Determination of Thermodynamic Data.*—Our earlier procedure<sup>1</sup> was followed for determining the stoichiometric stability constant  $K$  as a function of temperature for the various equilibria. Although equilibria (1) and (2) are clearly identifiable (Figure 2), their stoichiometric stability constants could not be determined with sufficient accuracy because of the proximity of the intense charge-transfer band whose edge commenced around 380 nm.

The chloro equivalent to equilibrium (3) had been studied<sup>1,2</sup> at various Cl:Ni mole ratios but no trends were noted. Table 1 contains a typical set of results for equilibrium (3). Table 2 summarizes the thermodynamic data determined as a function of Br:Ni mole ratio for equilibria (3)–(5), calculated for a typical temperature (403 K) and normalised to 293 K. Figure 6 shows plots of  $\log K$  against the reciprocal of the absolute temperature and their least-squares fits. Figure 7 reveals that, for the bromo system, there is a linear relationship between  $\Delta H$  and  $\log$  Br:Ni mole ratio for equilibrium (3).

## Discussion

The following nickel(II) halide (X) complexes have been reported in the literature<sup>3,6–11</sup> in non-aqueous solvents (sol):  $[\text{Ni}(\text{sol})_6]^{2+}$ ,  $[\text{NiX}(\text{sol})_5]^+$ ,  $[\text{NiX}_2(\text{sol})_4]$ ,  $[\text{NiX}_2(\text{sol})_2]$ ,  $[\text{NiX}_3(\text{sol})]^-$ , and  $[\text{NiX}_4]^{2-}$ . All types except  $[\text{NiCl}_2(\text{dmsO})_2]$  were found in the earlier work,<sup>1</sup> and the corresponding situation applies here. The spectra of the various chloro and bromo species are essentially similar, the latter having identical

**Table 2.** Thermodynamic data for equilibria (3)—(5) occurring in dmsO at various Br: Ni mole ratios. Data given at 403 K refer to a temperature around which most results were obtained; data at 293 K have been normalised to this standard temperature

Br: Ni mole ratio	$I/\text{mol dm}^{-3}$	403 K			293 K			$\Delta H/kJ \text{ mol}^{-1}$
		$\log_{10} K$	$\Delta G/kJ \text{ mol}^{-1}$	$\Delta S/J \text{ K}^{-1} \text{ mol}^{-1}$	$\log_{10} K$	$\Delta G/kJ \text{ mol}^{-1}$	$\Delta S/J \text{ K}^{-1} \text{ mol}^{-1}$	
Equilibrium (3)								
8.41	0.587	-1.119	8.64	259.2	-6.38	35.8	264	113.1
13.64	0.620	-0.434	3.36	228.2	-4.92	27.6	220	92.0
16.30	0.650	-0.359	2.52	197.8	-4.63	26.0	193	82.5
41.13	1.154	0.059	-0.41	166.6	-3.36	18.8	163	66.7
60.37	1.769	0.466	-3.59	160.3	-2.51	14.1	160	61.0
82.44	2.077	0.527	-4.05	127.1	-1.81	10.2	126	47.2
Equilibrium (4)								
154.4	2.860	1.50	-11.87	137.0	-5.42	30.4	45	43.7
Equilibrium (5)								
154.4	2.860	-0.332	2.55	-12.7	-0.33	1.9	-16	-2.7

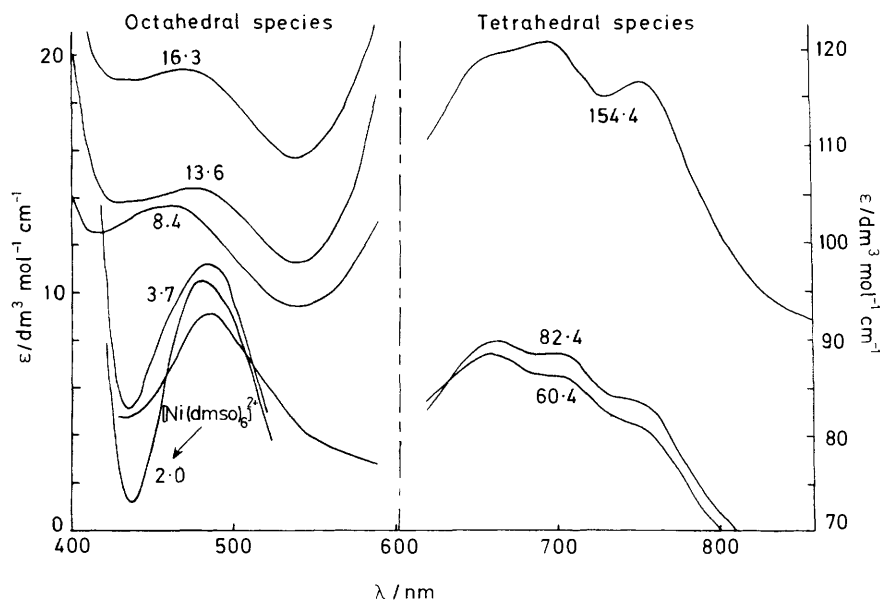


**Figure 5.** Effect of changing Br: Ni mole ratio [nickel(II) concentration constant] in dmsO at 130 °C. The molar absorptivity increased steadily in the 450–500 nm region as the spin-forbidden octahedral transition,  ${}^3A_{2g} \rightarrow {}^3T_{1g}(P)$ , of  $[\text{Ni}(\text{dmsO})_6]^{2+}$  loses some of its symmetry as dmsO is replaced by bromide; in the 600–800 nm region the spin-allowed bands of the  ${}^3T_1(F) \rightarrow {}^3T_1(P)$  transition of both tetrahedral species,  $[\text{NiBr}_3(\text{dmsO})]^-$  and  $[\text{NiBr}_4]^{2-}$ , are much more intense, and of approximately equal molar absorptivity

transitions but at lower energies, since bromide is below chloride, and both below dmsO, in the spectrochemical series. The arguments identifying the chloro complexes<sup>1</sup> will not be repeated here, only any differences and special features will now be given.

**Monobromo Complex,  $[\text{NiBr}(\text{dmsO})_5]^+$ .**—The band at 438 nm (Figure 2) is the  ${}^3A_{2g} \rightarrow {}^3T_{1g}(P)$  transition. Using  $[\text{Ni}(\text{dmsO})_6]^{2+}$  as reference, the band for monochloro complex has shifted 844  $\text{cm}^{-1}$  and that for the monobromo complex 1 270  $\text{cm}^{-1}$ . Also as expected, the molar absorptivity ( $\epsilon$ ) increased as the contiguous dmsO molecules were replaced by bromide (Figure 5).

**Dibromo Complex,  $[\text{NiBr}_2(\text{dmsO})_4]$ .**—The additional shift of the  ${}^3A_{2g} \rightarrow {}^3T_{1g}(P)$  transition upon replacement of a second solvent molecule by a second bromide is now less than the corresponding chloride case, but the total overall shift, relative

to  $[\text{Ni}(\text{dmsO})_6]^{2+}$ , is still greater, being 2 941  $\text{cm}^{-1}$  compared with 2 852  $\text{cm}^{-1}$ , and the molar absorptivity continues to increase.

**Tri- and Tetra-bromo Complexes,  $[\text{NiBr}_3(\text{dmsO})]^-$  and  $[\text{NiBr}_4]^{2-}$ .**—In the chloro system conditions were found where the spectra of both tetrahedral species could be recorded<sup>1,2</sup> but this was not possible here. Because higher temperatures were needed to generate equilibrium (3), complete conversion of all the nickel present to  $[\text{NiBr}_3(\text{dmsO})]^-$  had not occurred before the solution began to boil. And at the higher temperatures and Br: Ni mole ratios the conversion of  $[\text{NiBr}_3(\text{dmsO})]^-$  to  $[\text{NiBr}_4]^{2-}$  is incomplete because the equilibrium reversed. The individual profiles therefore cannot be recorded for these two species and those attributed in Figure 4 are derived spectra obtained as follows. The isosbestic point at 683 nm is, by definition, of fixed molar absorptivity, so the observed profiles passing through the point were adjusted; equal amounts

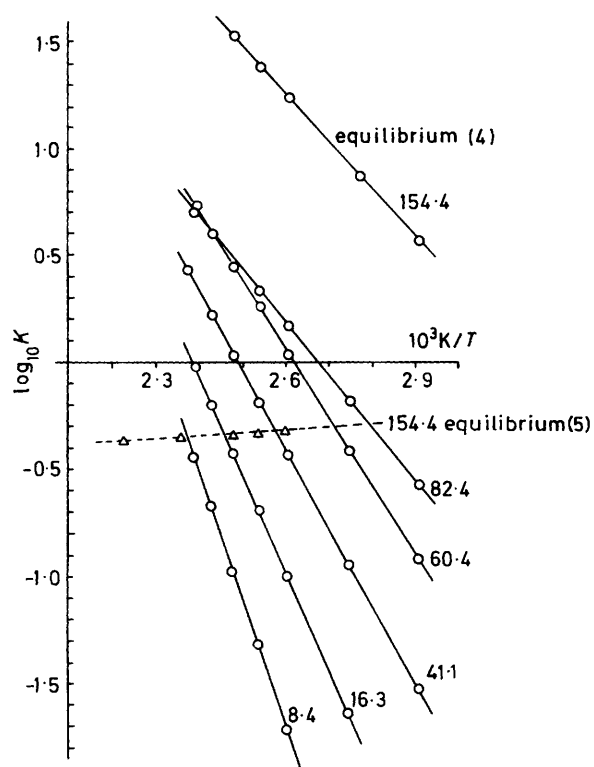


Figure 6. Plots of  $\log_{10} K$  vs. reciprocal temperature for various two-species equilibria (3)–(5) in dmsO with the Br:Ni mole ratio range of 8.4–154.4 (indicated)

were added to the low wavelength side and removed from the high wavelength side until the profile resembled that of  $[\text{NiCl}_3(\text{dmsO})]^-$ . The same, but opposite procedure, generated the spectrum of  $[\text{NiBr}_4]^{2-}$ . These profiles of  $[\text{NiBr}_3(\text{dmsO})]^-$  and  $[\text{NiBr}_4]^{2-}$  are reliable, since they compare well with those reported for  $[\text{NiBr}_3(\text{sol})]^-$  and  $[\text{NiBr}_4]^{2-}$  in the non-aqueous solvents acetone, tetrahydrofuran, dimethylacetamide, methyl ethyl ketone, acetonitrile and nitromethane by Fine<sup>11</sup> and other workers.<sup>6,7,9</sup> The extrapolated molar absorbance values ( $\epsilon$ ), at peak maxima, were however considerably less, as our spectra were not recorded at ambient but at elevated temperatures, which produces a general broadening and subsequent drop in peak height. Their accuracy is authenticated by the excellent linear plots of  $\log_{10} K$  against the reciprocal of the absolute temperature (Figure 6). In determining  $\Delta H$  for the three equilibria involving these species the  $K$  values were all obtained using extrapolated molar absorbance values,  $\epsilon$ .

At these elevated temperatures the  ${}^3T_1(F) \rightarrow {}^3T_1(P)$  of  $[\text{NiBr}_4]^{2-}$  comprises two bands at 755 and 704 nm, and a shoulder at 673 nm, close to the room-temperature values<sup>6,7,9,11</sup> of 753–755, 700–707, and 660–670 nm respectively. Replacement of one bromide ligand by a solvent ligand shifts this band system slightly. The reported distinctive features for  $[\text{NiBr}_3(\text{sol})]^-$  are, in all cases, bands at 700–715 and 643–656 nm, and a shoulder in the 610 nm region; we found for  $[\text{NiBr}_3(\text{dmsO})]^-$ , 702, 657, and 612 nm, respectively. The presence of one or both of these tetrahedral species in solution can thus be readily detected (Figures 4 and 5).

*Equilibria in Solution.*—We had previously proposed,<sup>1</sup> from our studies over a more limited range of Cl:Ni mole ratios, the reaction sequence given below (+ $T$  indicates an increase and  $-T$  a decrease in temperature). Our studies with the bromide system lead to a slightly different sequence. The

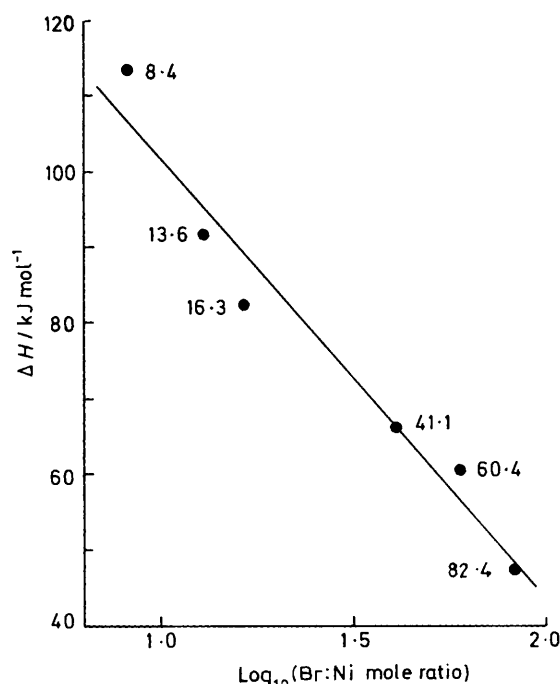
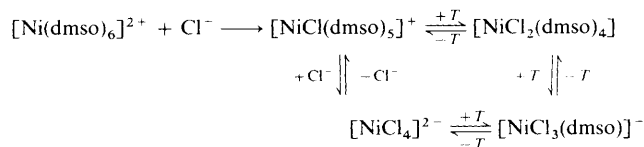
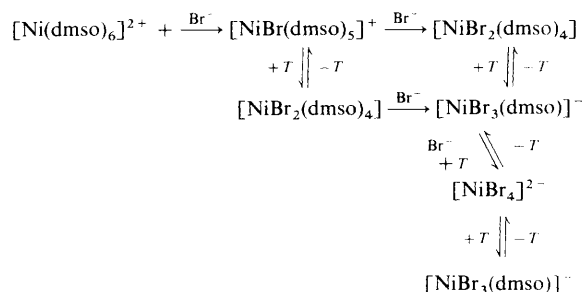


Figure 7. Plot of experimental  $\Delta H$  vs.  $\log_{10} (\text{Br:Ni mole ratio})$  for the equilibrium reaction in dmsO:  $[\text{NiBr}_2(\text{dmsO})_4]$  (octahedral) +  $\text{Br}^- \rightleftharpoons [\text{NiBr}_3(\text{dmsO})]^-$  (tetrahedral) + 3 dmsO. Numbers are Br:Ni mole ratios



Scheme 1.

experimental conditions for this reaction sequence are contained in Figure 1. In Scheme 2 the horizontal arrows in the top line indicate the species formed upon increasing the Br:Ni mole ratio at room temperature, and the vertical reversing arrows the effects of temperature change (as with the chloro system). The diagonal arrows indicate that tetrahedral  $[\text{NiBr}_4]^{2-}$  can only be formed in significant amounts from the tribromo species upon further addition of bromide and (limited) temperature increase. Once formed, a further temperature rise brings the system into an equilibrium regime where  $[\text{NiBr}_4]^{2-}$  forms  $[\text{NiBr}_3(\text{dmsO})]^-$  exothermically. Comparing the two systems, high Cl:Ni mole ratios yield<sup>1</sup>  $[\text{NiCl}_4]^{2-}$ ,  $[\text{NiCl}_3(\text{dmsO})]^-$ , and  $[\text{NiCl}(\text{dmsO})_5]^+$ , but not  $[\text{NiCl}_2(\text{dmsO})_4]$ , at



Scheme 2.

room temperature (Scheme 1 does not make this clear but it is demonstrated in Table 4 in the original work<sup>1</sup>). In contrast, the bromo system shows additionally  $[\text{NiBr}_2(\text{dmsO})_4]$  at ambient and requires both high Br:Ni mole ratios and high temperatures to form  $[\text{NiBr}_4]^{2-}$  and  $[\text{NiBr}_3(\text{dmsO})]^-$ .

**Thermodynamic Considerations.**—The isosbestic point at 550 nm (Figure 3), for reaction (3), exists over the widest range of temperature and Br:Ni mole ratios (8–82; Figure 1). The work on the chloro complexes<sup>1,2</sup> investigated the range of Cl:Ni mol ratios 3.28–9.65, and although the enthalpies determined for the di/tri-chloro equilibrium varied from 48 to 57 kJ mol<sup>-1</sup>, respectively, the errors involved precluded establishing a trend. However, Table 2 clearly shows trends in the thermodynamic data for this equilibrium reaction (and ionic strength data).

We attempted initially to relate  $\Delta H$  and ionic strength (which were in the range 0.5–2.0), and were unsuccessful, but subsequently found an excellent linear relationship between enthalpy and  $\log_{10}$  (Br:Ni mole ratio) (Figure 7). The correlation coefficient for this relationship is 0.992, and hence experimental (as distinct from standard) enthalpies, and other thermodynamic data, may be derived directly from this plot for the reaction  $[\text{NiBr}_2(\text{dmsO})_4] \rightleftharpoons [\text{NiBr}_3(\text{dmsO})]^-$ . Further work on the chloro system over a wider Cl:Ni mole ratio range may provide a similar trend, and predictive potential.

The thermodynamic data for the unique equilibria (4) and (5) are also included in Table 2. The conversion of  $[\text{NiBr}_3(\text{dmsO})]^-$  to  $[\text{NiBr}_4]^{2-}$  requires a little less energy than equilibrium (3), upon comparing the enthalpy for the latter (at the highest Br:Ni mole ratio used of 82.44) of 47.2 kJ mol<sup>-1</sup> with 43.7 kJ mol<sup>-1</sup> for equilibrium (4), at ratio 154.4 (and the slopes are similar in Figure 6).

Equilibrium (5), on the other hand, was slightly endothermic ( $\Delta H = -2.7$  kJ mol<sup>-1</sup>, Figure 6). We explain this shifting back of the equilibrium position at higher temperatures as due to the reduction in dielectric constant of the medium with increasing temperature destabilising the doubly charged tetrabromo species in favour of the singly charged  $[\text{NiBr}_3(\text{dmsO})]^-$ . The entropy change for this reaction was negative,  $-16$  J K<sup>-1</sup> mol<sup>-1</sup>, as expected and much smaller than for the other equilibria, 120–260 J K<sup>-1</sup> mol<sup>-1</sup> (Table 2). The values of the thermodynamic functions for equilibria (4) and (5) are not equal in magnitude and opposite in sign, as might at first be expected, because the system is changing and the lower dielectric constant regime [equilibrium (5)] produces more ion pairs, which do not directly alter *d-d* spectra, but would be expected to produce different thermodynamic data to that arising from equilibrium (4).

For the chloro reaction  $[\text{NiCl}_2(\text{dmsO})_4]$  (octahedral)  $\rightleftharpoons$   $[\text{NiCl}_3(\text{dmsO})]^-$  (tetrahedral), the few values obtained for the stoichiometric formation constant, *K*, at a fixed temperature, suggested an increase with increasing Cl:Ni mole ratio: here our results clearly did so. However, our absolute values were *ca.* 100 times *less* in the same ratio range. In marked contrast, the suggested increase in enthalpy values with increase in mole ratio for the chloro system was here unambiguously reversed. At the lowest Br:Ni mole ratio,  $\Delta H$  (at 113 kJ mol<sup>-1</sup>) was double any chloro value (48–56 kJ mol<sup>-1</sup>), and at the highest ratio the value of  $\Delta H$  (at 47 kJ mol<sup>-1</sup>) was around the lowest chloro

value. The free energy values,  $\Delta G$ , were again greater, and showed the same reversal in trend; and the same applied to the entropy data.

## Conclusions

The nickel–bromine bond in dimethyl sulphoxide solvent is therefore, as expected, weaker than the nickel–chlorine bond, but the nickel–halogen interactions are not identical in this solvent. Thus  $[\text{NiBr}_2(\text{dmsO})_4]$  may additionally be formed at ambient temperatures, but not  $[\text{NiBr}_4]^{2-}$ . This latter species could also not be formed exclusively under any conditions of temperature and Br:Ni mole ratio, and this cannot be for steric reasons since  $[\text{NiBr}_4]^{2-}$  is well known in many non-aqueous solvents.<sup>6,7,9,11</sup> The unusual reversal of the equilibrium  $[\text{NiBr}_3(\text{dmsO})]^- + \text{Br}^- \rightleftharpoons [\text{NiBr}_4]^{2-} + \text{dmsO}$  with continued temperature increase may not be unique if our explanation involving dielectric constant decrease and consequent ion pairing is correct: further investigations employing high-boiling solvents over a large temperature range are thus indicated.

We would point out that the various equilibria and the thermodynamic data determined for this system could not be obtained by electrochemical measurements or any of the other conventional techniques for measuring stoichiometric (or thermodynamic) formation constants as a function of temperature. Thus to resolve some of the questions now raised a more detailed study of absorption spectra of the chloro system is needed: studies on the corresponding iodo system are in progress.

## Acknowledgements

We thank S.E.R.C. for the provision of the Applied Physics Cary 14 H spectrophotometer, and N. J. P. thanks the S.E.R.C. and the C.E.G.B., Scientific Services Department, North East Region, Harrogate, for a C.A.S.E. Studentship. We also thank Paul Higgins for assistance with the early stages of this study.

## References

- 1 T. R. Griffiths and R. K. Scarrow, *J. Chem. Soc. A*, 1970, 827.
- 2 T. R. Griffiths and P. J. Potts, *J. Chem. Soc., Dalton Trans.*, 1975, 344.
- 3 See, for example T. R. Griffiths and R. K. Scarrow, *Trans. Faraday Soc.*, 1969, **65**, 1427, 2567, 3179; T. R. Griffiths and D. C. Tracey, *J. Inorg. Nucl. Chem.*, 1971, **33**, 2113; J. R. Dickinson, T. R. Griffiths, and P. J. Potts, *ibid.*, 1975, **37**, 511; T. R. Griffiths and P. J. Potts, *ibid.*, 1975, **37**, 521; T. R. Griffiths and R. A. Anderson, *Inorg. Nucl. Chem. Lett.*, 1979, **15**, 41; *Inorg. Chem.*, 1979, **18**, 2506; *J. Chem. Soc., Dalton Trans.*, 1980, 205, 209; *J. Chem. Soc., Faraday Trans. 1*, 1984, 2361.
- 4 C. R. Boston and G. P. Smith, *J. Sci. Instrum.*, 1969, **2**, 543.
- 5 G. P. Smith and J. B. Brynstad, *J. Phys. Chem.*, 1968, **72**, 296.
- 6 N. S. Gill and R. S. Nyholm, *J. Chem. Soc.*, 1959, 3997.
- 7 C. Furlani and G. Morpurgo, *J. Phys. Chem. (Frankfurt)*, 1961, **28**, 93.
- 8 L. I. Katzin and E. Gebert, *J. Am. Chem. Soc.*, 1950, **72**, 5464.
- 9 F. A. Cotton, D. M. L. Goodgame, and M. Goodgame, *J. Am. Chem. Soc.*, 1961, **83**, 4161.
- 10 L. I. Katzin, *J. Chem. Phys.*, 1962, **36**, 3034.
- 11 D. A. Fine, *Inorg. Chem.*, 1965, **4**, 345.
- 12 V. Gutmann, *Co-ord. Chem. Rev.*, 1967, **2**, 239.

Received 14th August 1987; Paper 7/1501